

Evelyn W. Wang<sup>1,2</sup>, Li-Fen Liu<sup>1,2</sup>, Bernard Levin<sup>1,2</sup>, Catherine E. Gleason<sup>2</sup>, Ranya Odeh<sup>2</sup>, Frances Hamkins-Indik<sup>2</sup>, Cristina Molina<sup>3</sup>, Andreu Odena<sup>3</sup>, Peadar Cremin<sup>2</sup>, Pablo D. Garcia<sup>2</sup>, Jinshu Fang<sup>2</sup>, Andrew T. Bockus<sup>2</sup>, Siegfried S.F. Leung<sup>2</sup>, Luis Hernandez<sup>2</sup>, Breena Fraga-Walton<sup>2</sup>, Nathan J. Dupper<sup>2</sup>, Justin A. Shapiro<sup>2</sup>, Megan K. DeMart<sup>2</sup>, Jie Zheng<sup>2</sup>, Steven Xie<sup>2</sup>, Ming-Hsun Ho<sup>2</sup>, Constantine Kreatsoulas<sup>2</sup>, Rajinder Singh<sup>2</sup>, James B. Aggen<sup>2</sup>, Violeta Serra<sup>3</sup>, Michael C. Cox<sup>2</sup>, David J. Earp<sup>2</sup>, Marie Evangelista<sup>2</sup>

<sup>1</sup> Co-first authors, <sup>2</sup> Circle Pharma, South San Francisco, CA, <sup>3</sup> Vall d'Hebron Institute of Oncology, Barcelona, Spain

## BACKGROUND

- The cyclin-dependent kinase (CDK)-RB-E2F axis forms the core transcriptional machinery driving cell cycle progression. Alterations in *RB1* or other pathway members occur in many cancers resulting in heightened oncogenic E2F activity. The activity of E2F is regulated by RxL-mediated binding to the hydrophobic patch (HP) or RxL binding site of Cyclin A; blocking this interaction results in hyperactivation of E2F and synthetic lethality in E2F-addicted tumors.
- While mechanistically differentiated and potentially more selective than blocking CDK activity (e.g., CDK2 or CDK4 inhibitors), the cyclin A/E2F RxL interaction was deemed undruggable.
- Leveraging our MXMO™ platform, we discovered CID-078, a passively permeable, selective, and orally bioavailable macrocycle with dual cyclin A/B RxL inhibiting activity that demonstrates efficacy in multiple E2F-driven cancer indications.

## Figure 1. The MXMO™ drug discovery engine integrates computational and synthetic platforms to rapidly generate macrocycles that can be administered orally

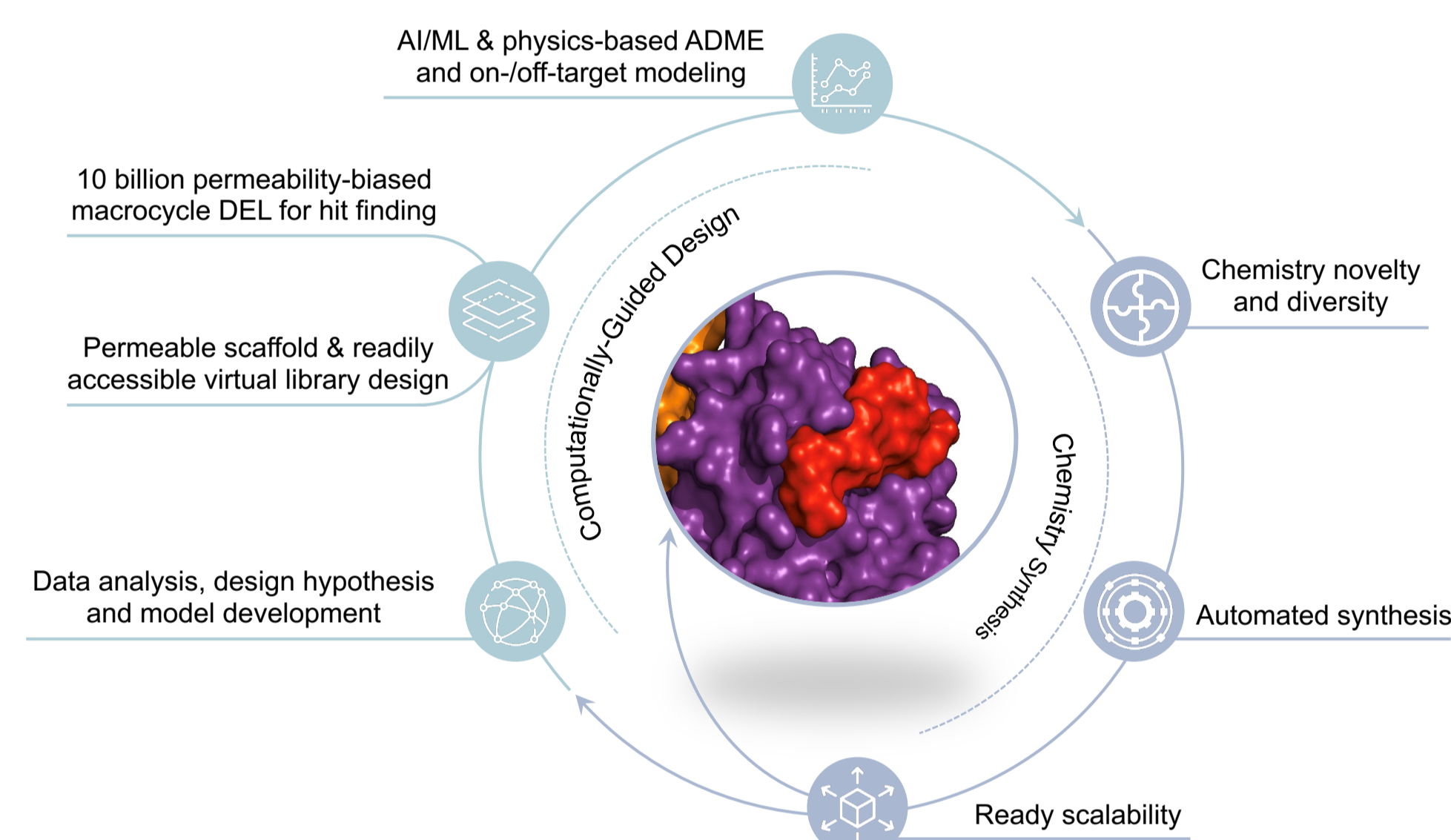


## Figure 2. MXMO™ has enabled the discovery of CID-078, a First-in-Class Oral Macrocyclic Cyclin A/B-RxL Inhibitor

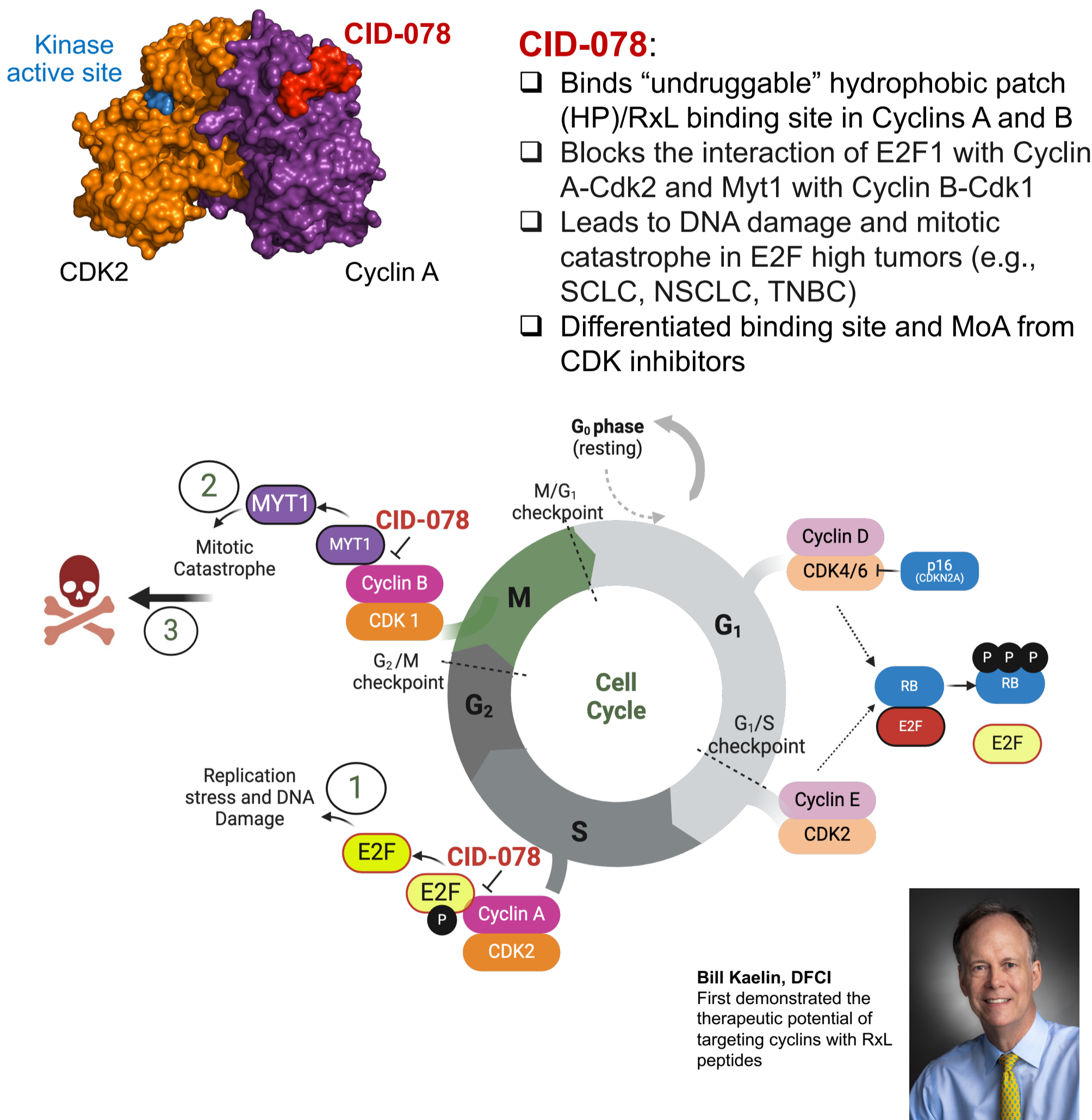


## Figure 3. CID-078 has activity across many tumor models

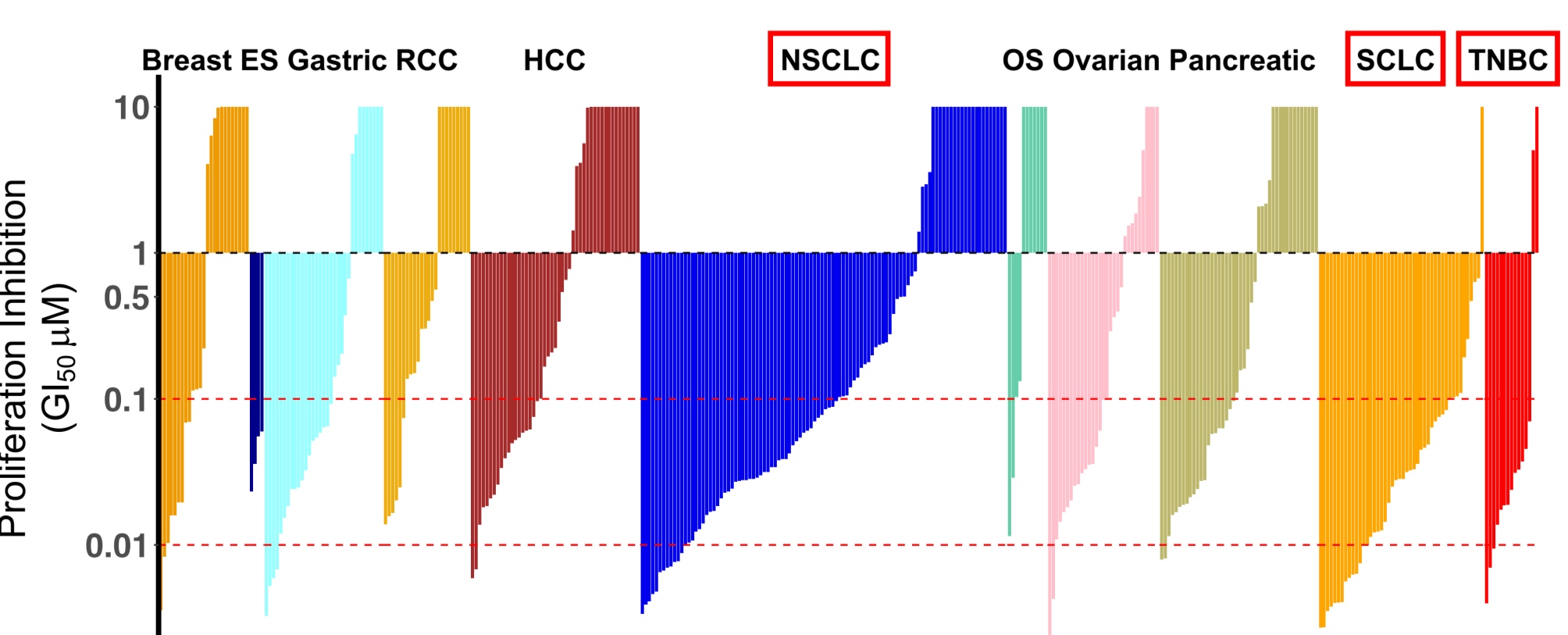


**Figure 3. GI<sub>50</sub> waterfall plots in response to CID-078.** CID-078 was profiled for anti-proliferation activity in a broad panel of cell lines representing various solid tumor indications. Cell lines were exposed to CID-078 for 4-8 days depending on length of time required for at least two cell doublings to occur. Cell growth inhibition was determined by Cell Titer Glo assay. ES, Ewing sarcoma; RCC, renal cell carcinoma; HCC, hepatocellular carcinoma; NSCLC, non-small cell lung cancer; OS, osteosarcoma; SCLC, small cell lung cancer; TNBC, triple negative breast cancer

## Results

### Figure 4. SCLC: CID-078 activity is associated with higher expression of E2F targets and the G2M checkpoint pathway

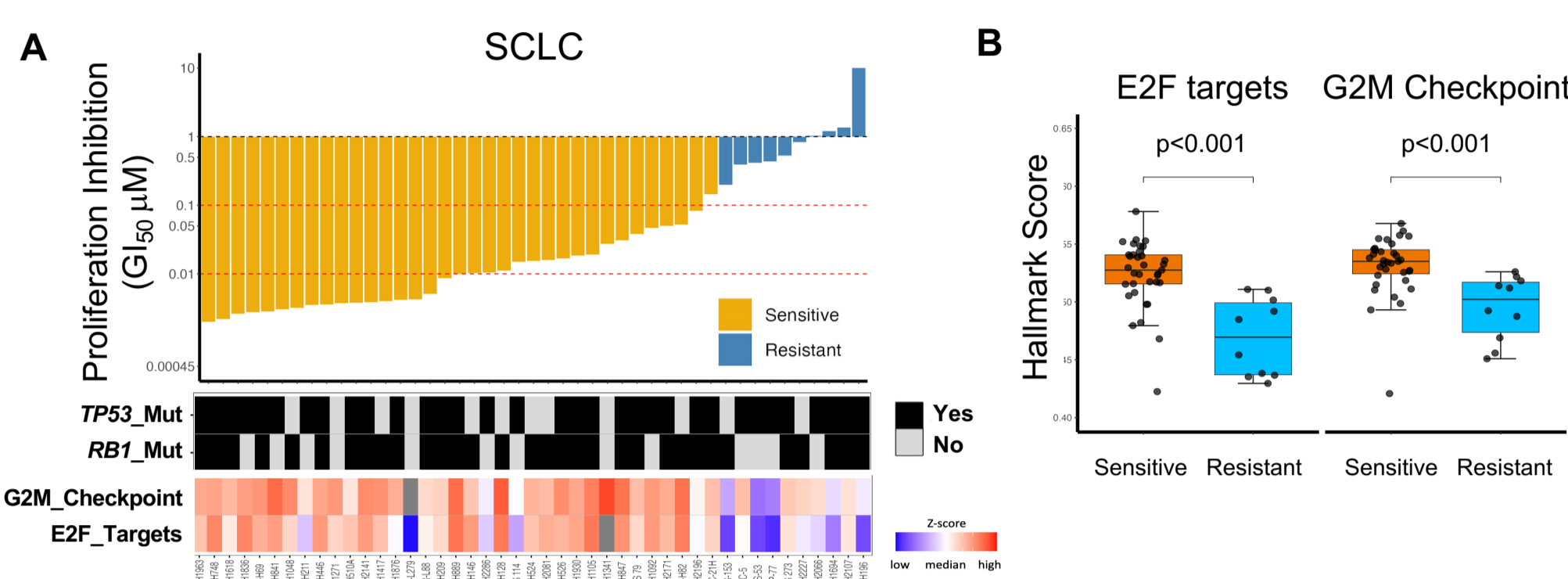


**Figure 4. (A)** Waterfall plots of sensitivity (GI<sub>50</sub>), genomic alteration status of *TP53* and *RB1*, and heatmaps of E2F targets and G2M checkpoint hallmark pathways Z-scores of 45 SCLC cell lines tested with CID-078. **(B)** E2F targets and G2M checkpoint hallmark pathway scores were associated with sensitivity to CID-078 in SCLC cell lines. Sensitivity is defined as GI<sub>50</sub> < 300 nM. P-values are shown and calculated by the Wilcoxon rank sum exact test.

### Figure 5. NSCLC: CID-078 activity trends with *RB1* status

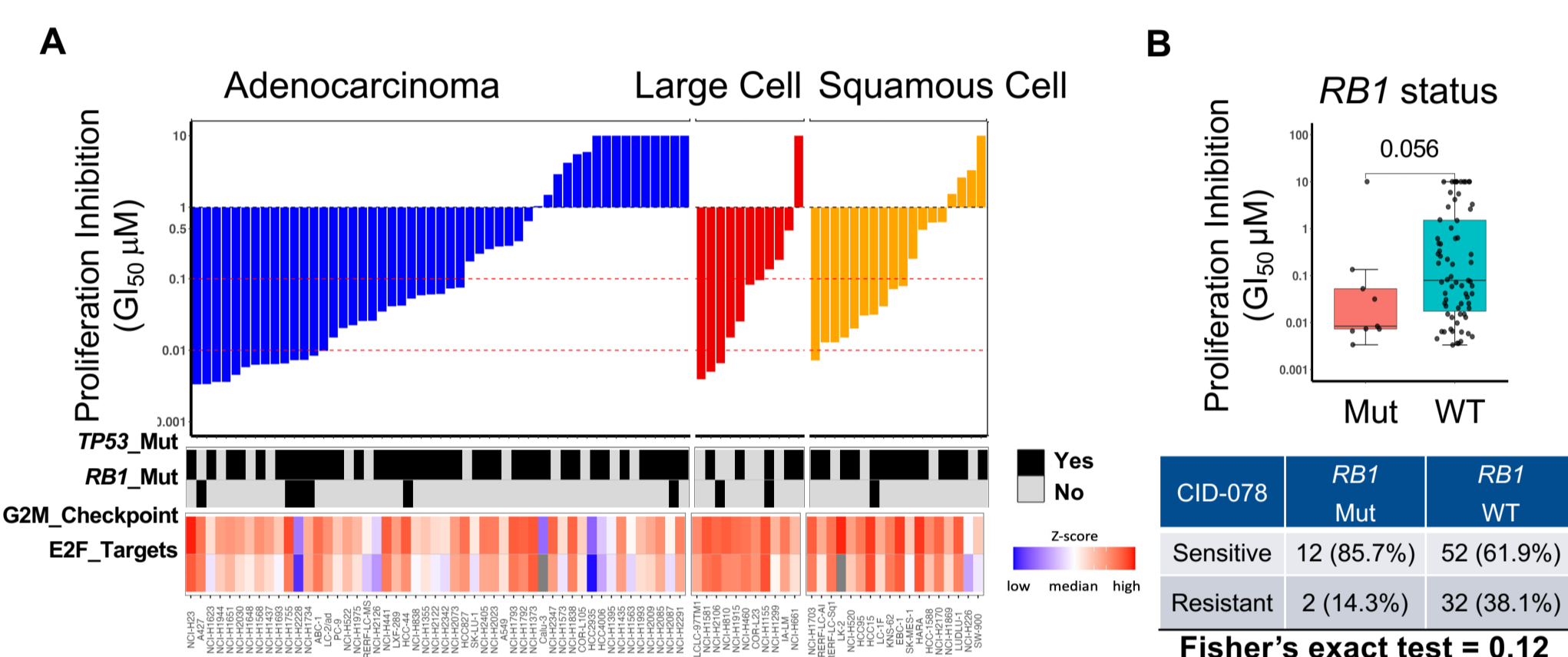


**Figure 5. (A)** Waterfall plots of sensitivity (GI<sub>50</sub>), genomic alteration status of *TP53* and *RB1*, and heatmaps of E2F targets and G2M checkpoint hallmark pathways Z-scores of 98 NSCLC cell lines tested with CID-078. **(B)** *RB1* status based on DNA alterations trended with sensitivity to CID-078 in NSCLC cell lines. P-values are shown and calculated by the Mann-Whitney or Fisher's exact test.

### Figure 6. Breast Cancer: TNBC shows higher expression of E2F targets and sensitivity to CID-078

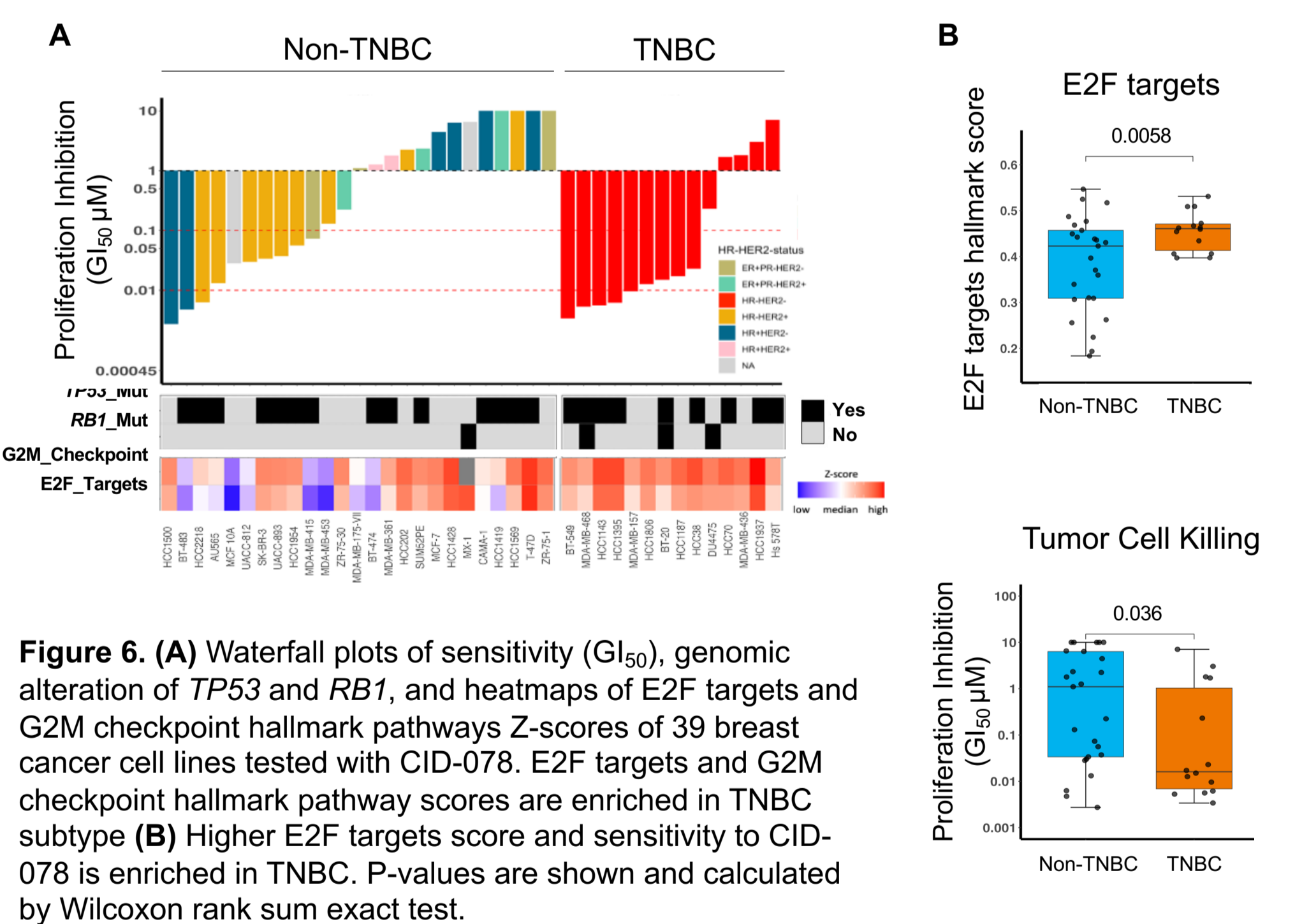


### Figure 7. CID-078 shows robust single agent activity and modulation of mitosis specific candidate biomarker p-separase in SCLC and NSCLC CDX/PDX models

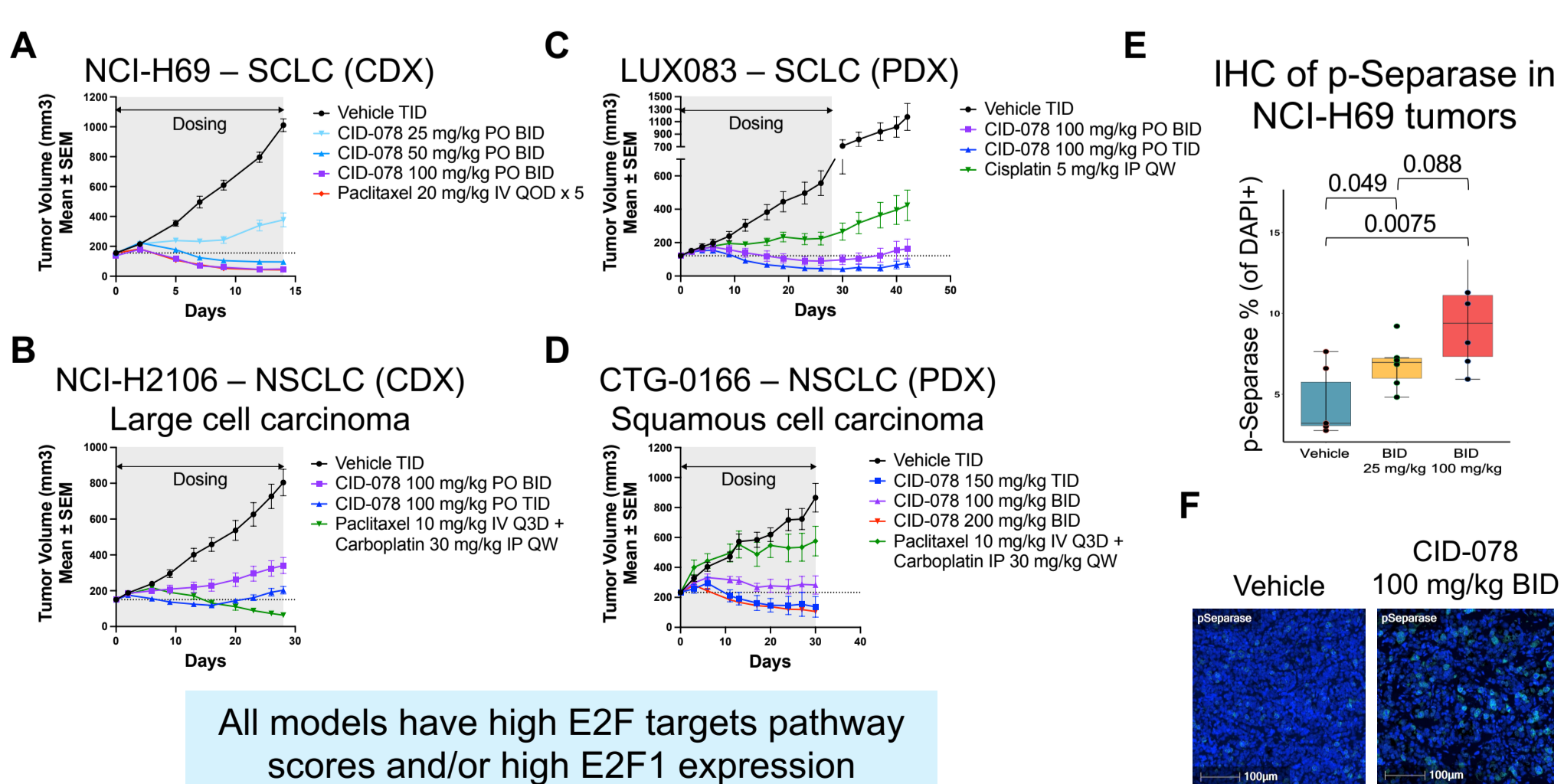


**Figure 7. In vivo SCLC and NSCLC xenograft studies.** Mice were inoculated SC with 5x10<sup>6</sup> NCI-H69 (A) or 1x10<sup>7</sup> NCI-H2106 (B) CDX cells, or fragments of LUX083 (C) or CTG-0166 (D) PDX tumors. Treatment was initiated when tumors reached 100-250 mm<sup>3</sup>. CID-078 and controls were administered at the doses indicated. All treatment regimens were tolerated as assessed by body weight measurements (not shown). Efficacy results for NCI-H69 represent two studies where controls behaved consistently. NCI-H69 tumors were collected after six days of treatment and stained for p-separase (S1126). Quantitation of positive cells as a percentage of DAPI+ cells (E) and representative images (F) are shown.

SC, subcutaneous; PO, orally; BID, twice daily; TID, three times daily; QOD, once every two days; Q3D, once every three days; QW, once weekly; SEM, standard error of mean

### Figure 8. CID-078 shows robust single agent activity in a TNBC *RB1* mutant PDX model and a luminal HR+/HER2-post-CDK4/6 inhibitor BC PDX model

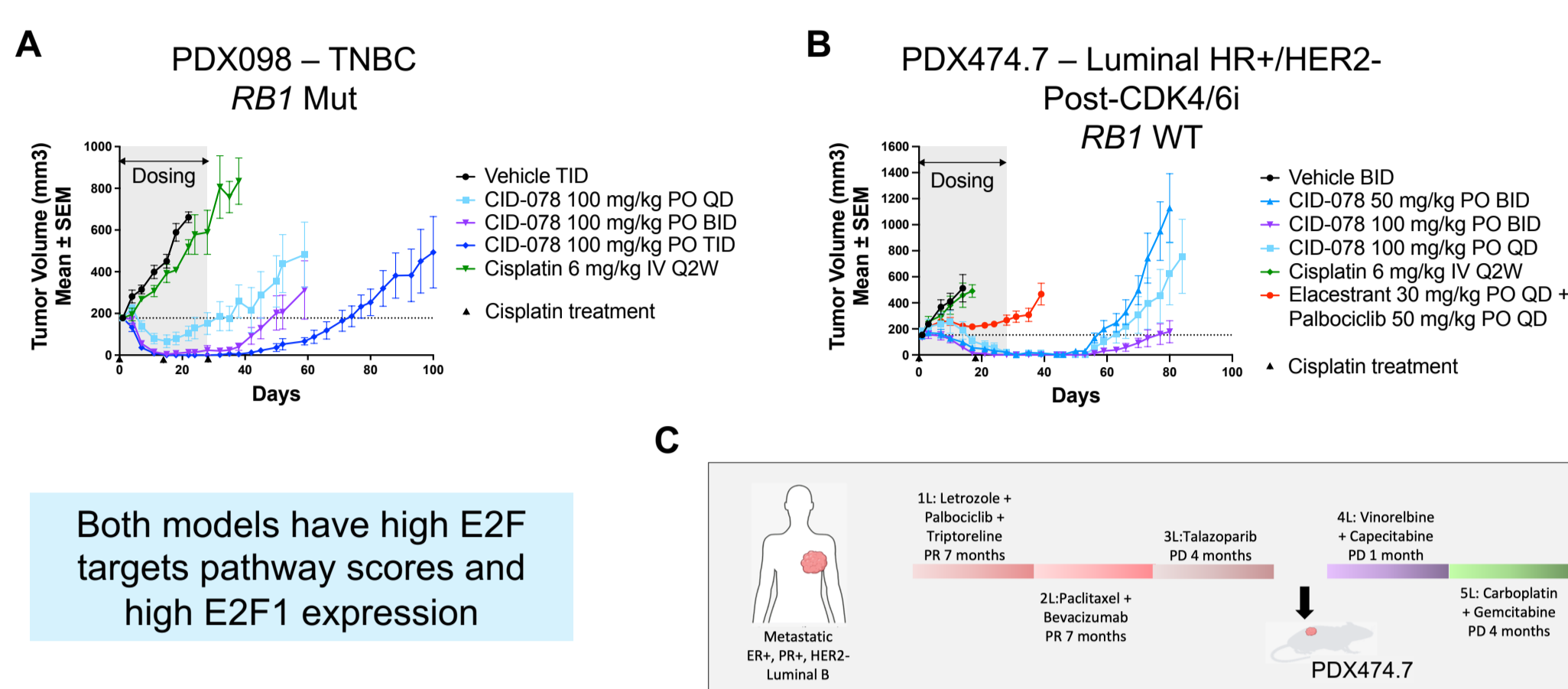


**Figure 8. In vivo breast cancer xenograft studies.** Mice were inoculated SC with fragments of PDX098 (A) or PDX474.7 (B) PDX tumors. Treatment was initiated when tumors reached 100-300 mm<sup>3</sup>. CID-078 and controls were administered at the doses indicated. All treatment regimens were tolerated as assessed by body weight measurements (not shown). Patient clinical history for PDX474.7 is shown (C).

SC, subcutaneous; PO, orally; QD, once daily; BID, twice daily; TID, three times daily; Q2W, once every two weeks; SEM, standard error of mean; PR, partial response; PD, progressive disease

### Figure 9. CID-078 shows single agent activity in CDK-RB-E2F dysregulated tumors

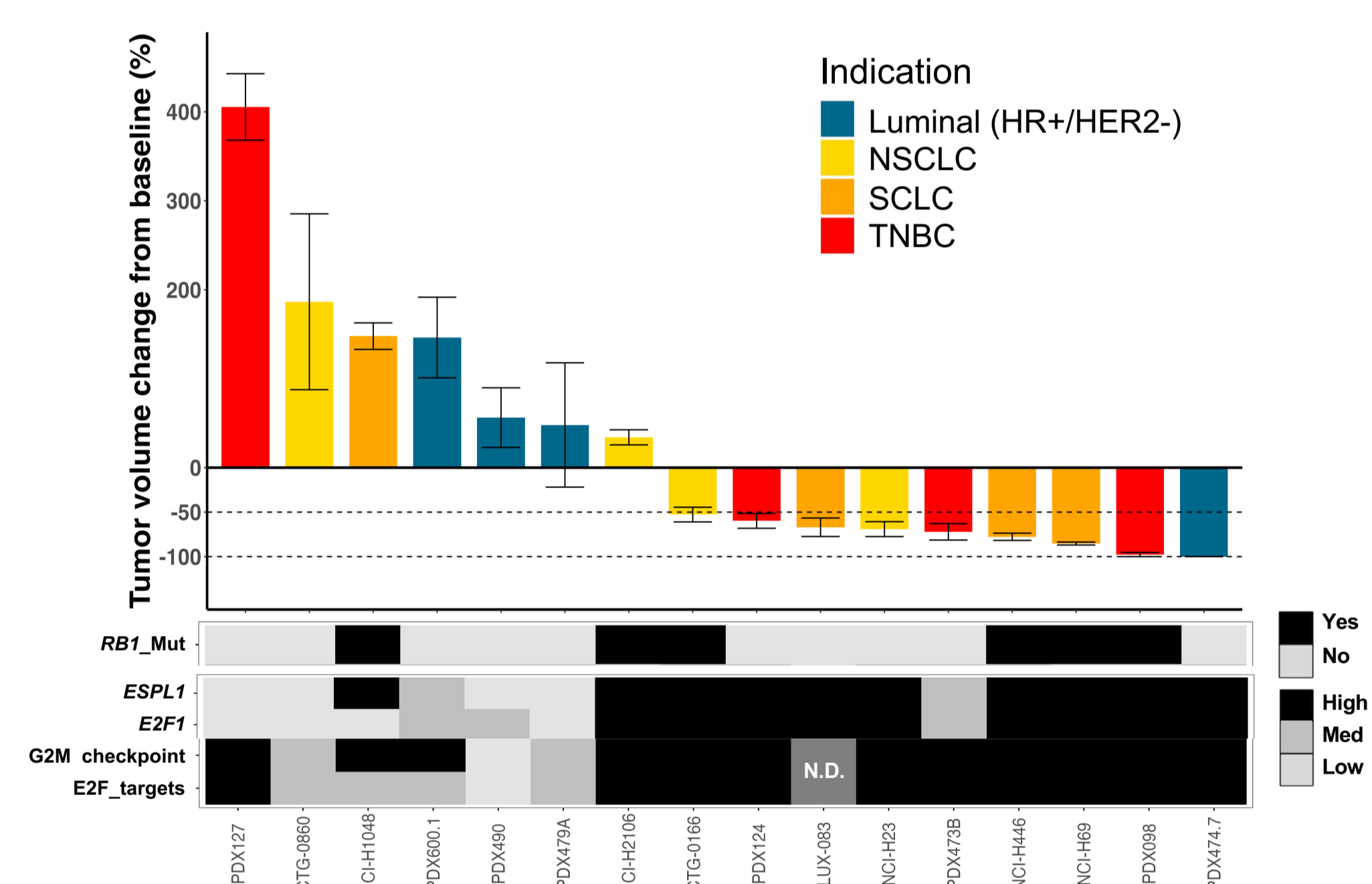


**Figure 9. Waterfall plot of in vivo efficacy data.** Best responses from SCLC, NSCLC, and breast CDX and PDX models is shown along with *RB1* genomic alteration status, *ESPL1* (separate) and *E2F1* gene expression, and G2M checkpoint and E2F hallmark pathway scores. Results for PDX127, PDX124, PDX473B, PDX098, and PDX474.7 are with 100 mg/kg BID dosing of CID-078. Results for CTG-0860, NCI-H1048, PDX600.1, PDX490, PDX479A, NCI-H2106, LUX083, NCI-H23, NCI-H446, and NCI-H69 are with 100 mg/kg TID dosing of CID-078. Results for CTG-0166 are with 200 mg/kg BID dosing of CID-078. N.D., no data.

### Figure 10. Now enrolling - CID-AB1-24001 (NCT06577987)

- Phase 1 dose escalation followed by dose expansion
- BOIN-BF design
- Oral dosing
- Pilot food-effect study included
- Primary endpoints: safety, tolerability, PK
- Primary outcome: recommended dose(s) for expansion
- First cohort enrolled
- Currently open sites: START Midwest, START Mountain, NEXT San Antonio
- Key Inclusion Criteria**
  - Adults with locally advanced or metastatic solid malignancy
  - RECIST v1.1 measurable disease (for patients with NSCLC, SCLC and patients with BC in backfill cohort) or evaluable disease
  - Able to swallow capsules and comply with study requirements
- Key Exclusion Criteria**
  - Unresolved ≥Grade 2 toxicity from previous tx, except chronic/stable toxicities
  - Brain metastases or spinal cord compression, unless treated and stable
  - Malabsorption or conditions that may interfere with absorption of product

## Conclusions

- The pre-clinical data for CID-078 provide compelling proof of concept for CID-078's potential as a novel and differentiated treatment for E2F-driven cancers.
- These data, along with suitable physical and pharmacokinetic properties and established nonclinical safety margins, supported progression of CID-078 into clinical studies.
- A multi-center phase 1 clinical trial (NCT06577987) is currently enrolling patients.

